

Design of Core-Pd/Shell-Ag Nanocomposite Catalyst for Selective Semihydrogenation of Alkynes

Takato Mitsudome, Teppei Urayama, Kenji Yamazaki, Yosuke Maehara, Jun Yamasaki, Kazutoshi Gohara, Zen Maeno, Tomoo Mizugaki, Koichiro Jitsukawa, and Kiyotomi Kaneda

ACS Catal., **Just Accepted Manuscript** • DOI: 10.1021/acscatal.5b02518 • Publication Date (Web): 22 Dec 2015

Downloaded from <http://pubs.acs.org> on December 28, 2015

Just Accepted

“Just Accepted” manuscripts have been peer-reviewed and accepted for publication. They are posted online prior to technical editing, formatting for publication and author proofing. The American Chemical Society provides “Just Accepted” as a free service to the research community to expedite the dissemination of scientific material as soon as possible after acceptance. “Just Accepted” manuscripts appear in full in PDF format accompanied by an HTML abstract. “Just Accepted” manuscripts have been fully peer reviewed, but should not be considered the official version of record. They are accessible to all readers and citable by the Digital Object Identifier (DOI®). “Just Accepted” is an optional service offered to authors. Therefore, the “Just Accepted” Web site may not include all articles that will be published in the journal. After a manuscript is technically edited and formatted, it will be removed from the “Just Accepted” Web site and published as an ASAP article. Note that technical editing may introduce minor changes to the manuscript text and/or graphics which could affect content, and all legal disclaimers and ethical guidelines that apply to the journal pertain. ACS cannot be held responsible for errors or consequences arising from the use of information contained in these “Just Accepted” manuscripts.

Design of Core-Pd/Shell-Ag Nanocomposite Catalyst for Selective Semihydrogenation of Alkynes

Takato Mitsudome,[†] Teppei Urayama,[†] Kenji Yamazaki,[‡] Yosuke Maehara,[‡] Jun Yamasaki,[§]
Kazutoshi Gohara,[‡] Zen Maeno,[†] Tomoo Mizugaki,[†] Koichiro Jitsukawa,[†] Kiyotomi Kaneda^{*,†,1}

[†] Department of Materials Engineering Science, Graduate School of Engineering Science and ¹
Research Center for Solar Energy Chemistry, Osaka University, 1-3, Machikaneyama, Toyonaka,
Osaka 560-8531, Japan

[‡] Division of Applied Physics, Graduate School of Engineering, Hokkaido University, Kita 13,
Nishi 8, Kita-Ku, Sapporo 060-8628, Japan

[§] Research Center for Ultra-High Voltage Electron Microscopy, Osaka University, 7-1,
Mihogaoka, Ibaraki, Osaka 567-0047, Japan

Abstract

We designed core-Pd/shell-Ag nanocomposite catalyst (Pd@Ag) for highly selective semihydrogenation of alkynes. The construction of the core-shell nanocomposite enables a significant improvement in the low activity of Ag NPs for the selective semihydrogenation of alkynes because hydrogen is supplied from the core-Pd NPs to the shell-Ag NPs in a synergistic manner. Simultaneously, coating the core-Pd NPs with shell-Ag NPs results in efficient suppression of overhydrogenation of alkenes by the Pd NPs. This complementary action of core-Pd and shell-Ag provides high chemoselectivity toward a wide range of alkenes with high Z-selectivity under mild reaction conditions (room temperature and 1 atm H₂). Moreover, Pd@Ag can be easily separated from the reaction mixture and is reusable without loss of catalytic activity or selectivity.

Keyword

core-shell, silver, palladium, semihydrogenation, alkyne

Text

Nano-structured composites with a core (inner material) and shell (outer layer) structure, so-called core-shell materials, have attracted enormous attention as highly

1
2
3
4
5
6 functionalized nanoarchitectures in diverse areas such as sensors¹, quantum dots²,
7 photonic crystals³, and catalysts⁴. The extensive study on design of core-shell materials
8 stems from their own intriguing characteristics, including optical, electronic, and
9 chemical properties. In the field of the catalyst design, core-shell nanoparticles have
10 exhibited unique and promising properties, such as high stability against sintering^{4d},
11 high activity through maximization of core-shell interfacial interaction^{4b}, and
12 multi-functionalized catalysis for one-pot tandem reaction through accumulation of
13 different active species in the core and shell^{4c}. Fine-tuning the composition and
14 morphology of such composites will enable rational design of novel core-shell
15 nanoparticle catalysts with fascinating tailored activities.

16
17
18
19
20
21
22 The semihydrogenation reaction, which converts alkynes to alkenes, is one of the
23 most important and fundamental reactions in manufacturing processes of bulk and fine
24 chemicals⁵. In this context, Lindlar catalyst (Pd/CaCO₃ treated by Pb salts) has been a
25 good first port of call in the synthesis of diverse alkenes⁶. However, the Lindlar catalyst
26 has serious drawbacks such as high toxicity of Pb species and the low alkene selectivity
27 when employing terminal alkynes due to the rapid overhydrogenation of terminal
28 alkenes to alkanes. Therefore, the development of the alternative Pb-free catalysts using
29 Pd⁷, Ni⁸, Cu⁹, Ru¹⁰ and Au¹¹ have been extensively studied.

30
31
32
33
34 It is well known that unmodified Pd NPs inherently shows high catalytic activity for
35 hydrogenation of alkynes, but low selectivity for alkenes due to overhydrogenation. In
36 contrast, Ag NPs has extremely low catalytic activity for semihydrogenation, requiring
37 high temperature or high H₂ pressure, despite intrinsically showing high
38 alkene-selectivity due to the rather weak complexation of Ag with alkenes¹². In
39 consideration of beneficial properties of Pd and Ag NPs, we anticipated that the
40 construction of a bimetallic core-shell nanocomposite catalyst consisting of Pd NPs in
41 the core and Ag NPs in the shell (Pd@Ag) would address the trade-off between activity
42 and selectivity for Pd and Ag NPs in semihydrogenation. Our design concept of Pd@Ag
43 represents the building of a compatible relationship between Pd, with its high activity,
44 and Ag, with its high alkene-selectivity, by construction of a core-shell structure. Pd
45 NPs in the core store hydrogen to form palladium-hydride (PdH)¹³ through the
46 H₂-permeable Ag shell nano-layer¹⁴. The inner PdH serves hydrogen to the outer Ag
47 shell, providing the Pb-free and selective semihydrogenation of alkynes occurring on
48 the Ag surface. Simultaneously, coating the Pd NPs by a Ag layer results in efficient
49 suppression of the overhydrogenation of alkenes at the Pd surface. This complementary
50 action of Pd and Ag, in which the advantages of Pd and Ag are integrated while their
51
52
53
54
55
56
57
58
59
60

disadvantages are remedied in a synergistic manner, allows selective semihydrogenation under mild reaction conditions (Figure 1).

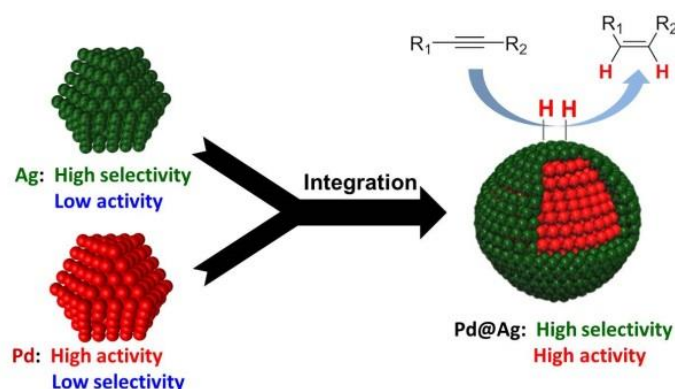


Figure 1 Design concept of complementary bimetallic core-Pd/shell-Ag catalyst for selective semihydrogenation of alkynes

Pd@Ag was synthesized by the seeding method (for details, see Supporting Information). Pd NPs with a mean diameter of 24.1 ± 5.7 nm were synthesized by reduction of Pd(acac)₂ in the presence of polyvinyl alcohol (PVA), with ethylene glycol as a solvent and reducing reagent. Next, the resulting Pd NPs were used as seeds for the formation of Pd@Ag by reduction of AgNO₃, with different Ag/Pd ratios (Ag/Pd = 0.10, 0.15, 0.20, 0.25, 0.50), using ascorbic acid in water. Hereafter, the resulting Pd@Ag catalysts are denoted Pd@Ag-X, where X is the Ag/Pd ratio.

Representative images of Pd@Ag-0.20 observed by transmission electron microscopy (TEM) and high-angle annular dark-field STEM (HAADF-STEM) are depicted in Figure 2. It can be seen that the NPs had a mean diameter of 26.2 ± 5.7 nm (Figure 2a). In the HAADF-STEM image of Pd@Ag, well-defined lattice fringes were observed (Figure 2b). The detected lattice fringes had d-spacing attributed to Ag {111} (2.36 Å) and Ag {200} (2.04 Å). This fact indicates that crystalline Ag grows on the surface of Pd NP seed. The elemental distribution of Ag on the Pd NPs in Pd@Ag (Figure 2c) was examined by scanning TEM (STEM) coupled with energy-dispersive X-ray spectroscopy (EDX) (Figures 2d, e, and f). Elemental mapping of Pd@Ag based on quantification analysis of EDX spectra clearly revealed that it comprised Pd NPs in the core and a nano-layer of Ag with a thickness of ca. 1 nm in the shell. The formation of a thin shell of Ag was also supported by XRD analysis, as no peak attributed to the formation of Ag nanoparticles or an alloy of Ag and Pd was observed around 35–50°

(Figure S11).

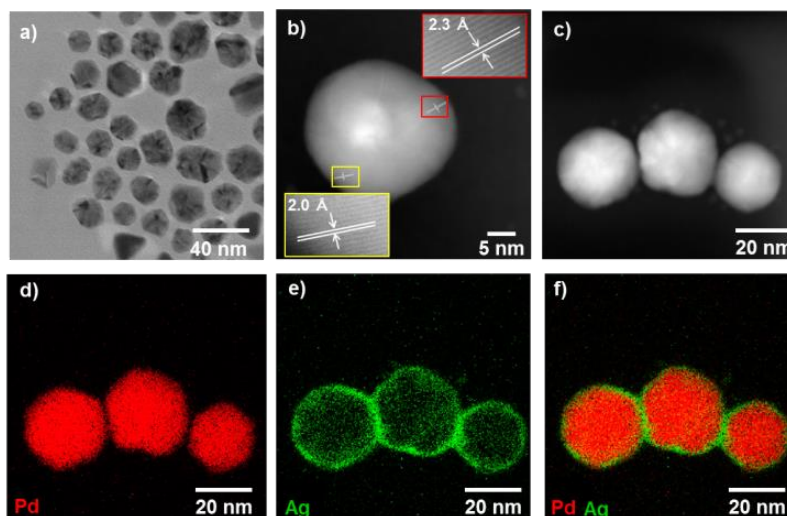


Figure 2 Composition and structural analysis of Pd@Ag-0.20. a) TEM image. b) and c) HAADF-STEM images. Elemental mapping images of d) Pd and e) Ag. f) Composite overlay image formed from d) and e).

After loading onto hydroxyapatite (HAP) which was chosen due to easy handling and to ensure high dispersion, the Pd@Ag-X composites were used as catalysts in the batchwise semihydrogenation of 1-octyne (**1**) at room temperature under atmospheric pressure of H₂¹⁵. In order to compare catalytic activity, both single Pd NPs (Pd seed for Pd@Ag) and Ag NPs loaded on HAP were prepared. The results are shown in Table 1. Pd NPs promoted rapid overhydrogenation, quantitatively giving the undesired product *n*-octane (**3**) (Table 1, Entry 1). Ag NPs did not show any catalytic activity under the conditions used (Table 1, Entry 2). As previously reported^{12b}, highly alkene-selective catalysis of Ag NPs was confirmed under high pressure of H₂ (50 atm), although with extremely low activity (turnover frequency = 0.035 h⁻¹) (Table 1, Entry 3). In contrast, the various Pd@Ag-X composites showed differing activity and selectivity toward **2** depending on the value of X. When the Ag/Pd ratio X was increased from 0.10 to 0.20, alkene-selectivity steadily increased (Table 1, Entries 4–6), with Pd@Ag-0.20 exhibiting the highest catalytic activity, affording **2** in quantitative yield (Table 1, Entry 6). Upon a further increase in the Ag/Pd ratio to 0.50, complete alkene-selectivity was retained but the activity of the catalyst gradually decreased (Table 1, Entries 8 and 9). Interestingly, the excellent alkene-selectivity of Pd@Ag-0.20 was maintained even when the reaction time was prolonged after full conversion of **1** (Figure S16). Notably, the C=C bond of **2** remained almost intact up to a H₂ pressure of 50 atm (Table 1, Entry

7). This high performance of Pd@Ag-0.20 arising from the core-shell structure is in sharp contrast with many previous catalysts, including the Lindlar catalyst and Pd-Ag alloys, which easily causes overhydrogenation of terminal alkenes to alkanes¹⁶.

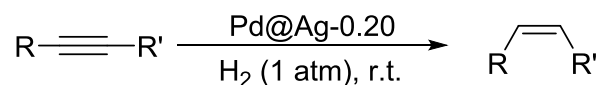
Table 1 Semihydrogenation of **1** using various Pd-Ag catalysts

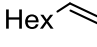
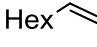
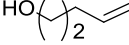
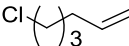
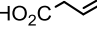
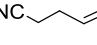
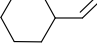
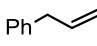
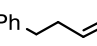
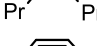
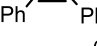
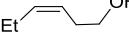
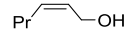
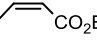
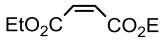
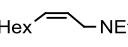
Hex-1-yn-5-ene (1) $\xrightarrow[\text{H}_2 (1 \text{ atm}), \text{ r.t.}]{\text{Catalyst}}$ Hex-1-en-5-ene (2) + Hexane (3)

Entry	Catalyst	Time [h]	Conv. [%] ^a	2 [%] ^a	3 [%] ^a
1	Pd NPs	0.5	>99	0	>99
2 ^b	Ag NPs	2.5	0	-	-
3 ^c	Ag NPs	20	36	36	0
4	Pd@Ag-0.10	2.5	>99	23	76
5	Pd@Ag-0.15	2.5	>99	80	19
6	Pd@Ag-0.20	2.5	>99	>99	0
7 ^d	Pd@Ag-0.20	1.0	>99	>99	0
8	Pd@Ag-0.25	2.5	65	65	0
9	Pd@Ag-0.50	2.5	22	22	0

Reaction conditions: Catalyst (0.10 g, Pd: 0.33 mol%, Ag: 0.033 mol%-0.17 mol%), **1** (0.3 mmol), EtOH (2 ml). ^aDetermined by GC using internal standard technique. ^bAg/HAP (Ag: 0.33 mol%). ^cAg/HAP (Ag: 50 mol%), H₂ (50 atm). ^dH₂ (50 atm).

The catalytic potential of Pd@Ag-0.20, which exhibited the best performance, was investigated using various alkynes in a batch reactor. A wide range of terminal and internal alkynes containing functional groups such as hydroxyl, carboxylic acid, ester, amine, cyano, and halogen groups were smoothly converted to the corresponding alkenes with >99% selectivity (Table 2). After the reaction, the Pd@Ag catalyst loaded onto HAP was easily recovered by filtration, and proved to be reusable, retaining its high activity and selectivity during five recycling experiments, which demonstrates its high durability (Table 2, Entry 2). We also examined the practical utility of Pd@Ag by using a plug flow reactor for gram-scale synthesis. When **1** (10 mmol, 1.10 g) in ethanol (0.10 M) was passed through a Pd@Ag-0.20-packed column reactor at a flow rate of 4.2 mL h⁻¹ along with H₂ at atmospheric pressure, **2** was successively obtained in over 99% yield (96% isolated yield; 1.07 g).

Table 2 Semihydrogenation of various alkynes

Entry	Product	Time [h]	Conv. [%] ^a	Yield [%] ^a	<i>E/Z</i> [%] ^a
1		2.5	>99	>99 (95)	-
2 ^b		2.5	>99	>99	-
3		1.0	>99	>99 (93)	-
4		1.5	>99	>99 (91)	-
5		3.0	>99	>99 (92)	-
6		3.0	>99	>99 (93)	-
7 ^c		14	>99	>99 (92)	-
8		3.0	>99	>99 (96)	-
9		3.0	>99	>99 (95)	-
10		4.0	>99	>99 (94)	0/100
11		4.0	>99	>99 (98)	0/100
12		5.0	>99	>99 (94)	0/100
13		5.5	>99	>99 (94)	0/100
14		5.0	>99	>99 (91)	4/96
15 ^d		12	>99	>99 (92)	16/84
16		15	>99	>99 (93)	0/100

Reaction conditions: Pd@Ag-0.20 (0.10 g, Pd: 0.33 mol%, Ag: 0.066 mol%), alkyne (0.3 mmol), EtOH (2 mL). ^aDetermined by GC using internal standard technique. Values in parentheses are isolated yields. ^b5th reuse. ^cHexane (2 mL). ^d50 °C.

To elucidate the reasons for the significant differences in the performance of Pd@Ag-X depending on X, the shell effect of Ag was investigated by CO adsorption FTIR spectroscopy (Figure S13). It is well known that CO is not adsorbed onto the Ag NP surface but is strongly adsorbed on Pd NPs¹⁷. In fact, when single Ag NPs and Pd NPs were treated with CO, no CO adsorption peaks were observed for Ag NPs, while

1
2
3
4
5
6 two CO adsorption peaks derived from CO stretching at 1930 cm^{-1} and 2060 cm^{-1} were
7 observed for Pd NPs. IR spectra of Pd@Ag-0.10 and Pd@Ag-0.15 treated with CO
8 showed two peaks in the same position as for single Pd NPs. On the other hand, it is
9 notable that Pd@Ag-0.20, Pd@Ag-0.25, and Pd@Ag-0.50 showed no CO adsorption
10 peaks, demonstrating that the Pd NPs were entirely covered by Ag in a core-shell
11 structure. These results showed that the low alkene-selectivity of Pd@Ag-0.10 and
12 Pd@Ag-0.15 was strongly associated with the presence of the exposed Pd NPs, causing
13 overhydrogenation. The steadily decreasing activity of Pd@Ag-X as X increased from
14 0.20 to 0.50 was explained by the increase in thickness of the Ag shell, which hinders
15 the supply of hydrogen from the core-Pd NPs to the surface Ag sites. TEM images of
16 Pd@Ag supported the contention that the thickness of the Ag shell could be controlled
17 by changing the amount of Ag used. The mean diameters of Pd@Ag-X, where X was
18 0.10, 0.15, 0.20, 0.25, and 0.50, were 25.2 ± 4.0 , 25.9 ± 4.9 , 26.2 ± 5.7 , 26.6 ± 5.9 , and
19 27.0 ± 4.5 (Figure S1–S4, S6, and S7).

20
21 Among noble metals, Ag nanocrystals have uniquely bifunctional properties with not
22 only the alkene-selective catalysis but also the high activity for surface-enhanced
23 Raman spectroscopy (SERS), allowing in-situ monitoring of Ag-catalyzed surface
24 reaction. Therefore, we investigated the Pd@Ag-catalyzed semihydrogenation by SERS.
25 Figure 3(A) shows SERS spectra from ethanol suspension of Pd NPs and Pd@Ag in the
26 presence of phenylacetylene (PA) as a Raman probe. No peaks of PA (0.12 mM) without
27 nanoparticles or with Pd NPs were confirmed (Figure 3A (a) and (b)). Interestingly,
28 when the colloidal Pd@Ag was dropped into the ethanol solution of PA, new peaks at
29 1980 cm^{-1} ($\text{C}\equiv\text{C}$ stretching mode) and 1590 cm^{-1} (benzene ring mode) appeared,
30 demonstrating the SERS activity of Pd@Ag (Figure 3A (c)). The shift in the peak at
31 2111 cm^{-1} for the $\text{C}\equiv\text{C}$ stretching of free PA to 1980 cm^{-1} is assigned to surface
32 adsorption of PA on Ag (Figure 3A (c) vs. (d)), in agreement with previous finding¹⁸.
33 Moreover, the SERS activity of Pd@Ag enabled the in-situ monitoring of the
34 Pd@Ag-catalyzed semihydrogenation of PA. After adding Pd@Ag to the PA solution
35 under atmospheric H_2 conditions, the SERS spectrum was recorded (Figure 3B). The
36 peaks attributed to the PA adsorbed on the surface of Ag gradually decreased during the
37 semihydrogenation of PA, supporting that the semihydrogenation undergoes on the
38 surface of Ag shell of Pd@Ag where the Pd core serves as a hydrogen source due to the
39 formation of a PdH species. The formation of the PdH was confirmed by XRD analysis
40 (Figure S12) where the XRD peaks attributed to Pd core of Pd@Ag shifted to low-angle
41 side under H_2 atmosphere. Furthermore, the H_2 - D_2 exchange experiment using Ag NPs
42 catalyst (Scheme S2) revealed the formation of HD, indicating the possibility for
43
44
45
46
47
48
49
50
51
52
53
54
55
56
57
58
59
60

H₂-permeability of Ag shell.

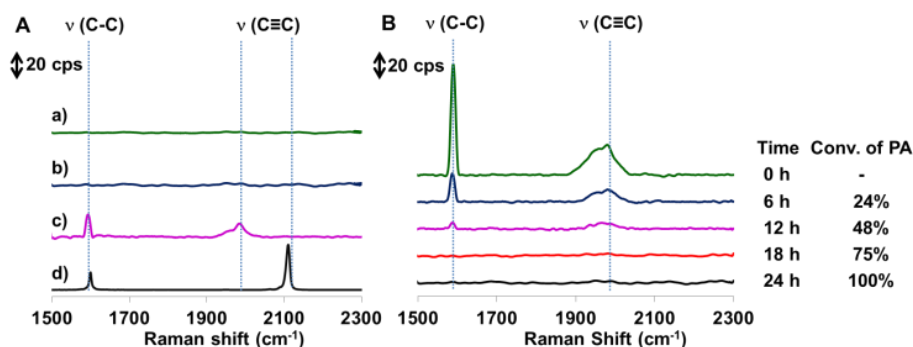


Figure 3 (A) Raman spectra recorded from ethanol suspension of nanoparticles in the presence of PA: a) 0.12 mM PA, b) 0.12 mM PA with Pd NPs, c) 0.12 mM PA with Pd@Ag-0.20 and d) reference PA (intensity: 1/500). (B) SERS spectra recorded during the semihydrogenation of PA catalyzed by Pd@Ag-0.20 at r. t. under 1 atm of H₂.

In conclusion, we designed core-Pd/shell-Ag nanocomposite catalysts (Pd@Ag) whose components acted in complementary fashion to achieve Pb-free and highly selective semihydrogenation of alkynes under mild reaction conditions. The Pd@Ag catalyst (loaded on HAP) was reusable and applicable to use in a plug flow reactor. It was found that the core-Pd enhanced the activity of the shell-Ag by serving as a hydrogen source, while, at the same time, the shell Ag reduced the intrinsically low alkene-selectivity of Pd by inhibiting contact between Pd and alkenes. As a whole, the complementary relationship between Pd and Ag derived from the core-shell arrangement resulted in highly active and selective catalysis in the semihydrogenation of alkynes.

Supporting Information

Experimental details and characterization of catalysts. This material is available free of charge via the Internet at <http://pubs.acs.org>.

AUTHOR INFORMATION

Corresponding Author

E-mail: Kaneda@cheng.es.osaka-u.ac.jp

Acknowledgement

This work was supported by JSPS KAKENHI Grant Nos. 26289303, 26630410, 26105003, and 24246129. This work was also supported by the Program for Creating Future Wisdom, Osaka University, selected in 2014. A part of this work was conducted in Hokkaido University, supported by Nanotechnology Platform Program of the Ministry of Education, Culture, Sports, Science and Technology (MEXT), Japan.

References

- [1] (a) Lim, D.-K.; Jeon, K.-S.; Kim, H. M.; Nam, J.-M.; Suh, Y. D. *Nat. Mater.* **2010**, *9*, 60-67. (b) Li, J. F.; Huang, Y. F.; Ding, Y.; Yang, Z. L.; Li, S. B.; Zhou, X. S.; Fan, F. R.; Zhang, W.; Zhou, Z. Y.; Wu, D. Y.; Ren, B.; Wang, Z. L.; Tian, Z. Q. *Nature* **2010**, *464*, 392-395. (c) Zhu, H.; Sigdel, A.; Zhang, S.; Su, D.; Xi, Z.; Li, Q.; Sun, S. *Angew. Chem. Int. Ed.* **2014**, *53*, 12508-12512.
- [2] (a) Rogach, A.; Susha, A.; Caruso, F.; Sukhorukov, G.; Kornowski, A.; Kershaw, S.; Möhwald, H.; Eychmüller, A.; Weller, H. *Adv. Mater.* **2000**, *12*, 333-337. (b) Ge, J.; Lee, H.; He, L.; Kim, J.; Lu, Z.; Kim, H.; Goebel, J.; Kwon, S.; Yin, Y. *J. Am. Chem. Soc.* **2009**, *131*, 15687-15694.
- [3] (a) Burns, A.; Ow, H.; Wiesner, U. *Chem. Soc. Rev.* **2006**, *35*, 1028-1042. (b) Smith, A. M.; Mohs, A. M.; Nie, S. *Nat. Nanotechnol.* **2009**, *4*, 56-63. (c) Makki, R.; Ji, X.; Mattoussi, H.; Steinbock, O. *J. Am. Chem. Soc.* **2014**, *136*, 6463-6469.
- [4] (a) Alayoglu, S.; Nilekar, A. U.; Mavrikakis, M.; Eichhorn, B. *Nat. Mater.* **2008**, *7*, 333-338. (b) Mitsudome, T.; Mikami, Y.; Matoba, M.; Mizugaki, T.; Jitsukawa, K.; Kiyotomi, K. *Angew. Chem. Int. Ed.* **2012**, *51*, 136-139. (c) Yang, Y.; Liu, X.; Li, X.; Zhao, J.; Bai, S.; Liu, J.; Yang, Q. *Angew. Chem. Int. Ed.* **2012**, *51*, 9164-9168. (d) Peng, H.; Xu, L.; Zhang, L.; Zhang, K.; Liu, Y.; Wu, H.; Wu, P. *J. Mater. Chem.* **2012**, *22*, 14219-14227. (e) Dhakshinamoorthy, A.; Garcia, H. *Chem. Soc. Rev.* **2012**, *41*, 5262. (f) Mitsudome, T.; Takahashi, Y.; Ichikawa, S.; Mizugaki, T.; Jitsukawa, K.; Kaneda, K. *Angew. Chem. Int. Ed.* **2013**, *52*, 1481-1485.
- [5] (a) Derrien, M. L. *Catalytic Hydrogenation, Stud. Surf. Sci. Catal. Vol. 27, Elsevier, Amsterdam*, **1986**, 613-640. (b) Piringner, O. G.; Baner, A. L. *Plastic Packaging: Interactions with Food and Pharmaceuticals*, Wiley, New Jersey, **2008**, 32-46.
- [6] Lindlar, H.; Dubuis, R. *Org. Synth. Coll.* **1973**, *5*, 880-882.
- [7] (a) Gruttadauria, M.; Natto, R.; Deganello, G.; Liotta, L. F. *Tetrahedron Lett.* **1999**, *40*, 2857-2858. (b) Sajiki, H.; Mori, S.; Ohkubo, T.; Ikawa, T.; Kume, A.; Maegawa, T.; Monguchi, Y. *Chem. Eur. J.* **2008**, *14*, 5109-5111. (c) Hori, J.; Murata, K.; Sugai, T.; Shinohara, H.; Noyori, R.; Arai, N.; Kurono, N.; Ohkuma, T. *Adv. Synth. Catal.* **2009**, *351*, 3143-3149. (d) Takahashi, Y.; Hashimoto, N.; Hara, T.; Shimazu, S.; Mitsudome,

- 1
2
3
4
5
6 T.; Mizugaki, T.; Jitsukawa, K.; Kaneda, K. *Chem. Lett.* **2011**, *40*, 405-407. (e) Chan, C.
7 W. A.; Xie, Y.; Cailuo, N.; Yu, K. M. K.; Cookson, J.; Bishop, P.; Tsang, S. C. *Chem.*
8 *Commun.* **2011**, *47*, 7971-7973. (f) Yabe, Y.; Yamada, T.; Nagata, S.; Sawara, Y.;
9 Monguchi, Y.; Sajiki, H. *Adv. Synth. Catal.* **2012**, *354*, 1264-1268. (g) Lee, Y.;
10 Motoyama, Y.; Tsuji, K.; Yoon, S.-H.; Mochiba, I.; Nagashima, H. *ChemCatChem* **2012**,
11 *4*, 778-781. (h) Yabe, Y.; Sawama, Y.; Monguchi, Y.; Sajiki, H. *Catal. Sci. Technol.* **2014**,
12 *4*, 260-271. (i) Slack, E. D.; Gabriel, C. M.; Lipshutz, B. H. *Angew. Chem. Int. Ed.* **2014**,
13 *53*, 14051-14054.
14
15 [8] (a) Brown, C. A.; Ahuja, V. K.; *J. Chem. Soc. Chem. Commun.* **1973**, *15*, 553-554.
16 (b) Studt, F.; Abild-Pedersen, F.; Bligaard, T.; Sørensen, R. Z.; Christensen, C. H.;
17 Nørskov, J. K. *Science* **2008**, *320*, 1320-1322.
18 [9] Semba, K.; Fujihara, T.; Xu, T.; Terao, J.; Tsuji, Y. *Adv. Synth. Catal.* **2012**, *354*,
19 1542-1550.
20 [10] Niu, M.; Wang, Y.; Li, W.; Jiang, J.; Jin, Z. *Catal. Commun.* **2013**, *38*, 77-81.
21 [11] (a) Shao, L.; Huang, X.; Teschner, D.; Zhang, W. *ACS Catal.* **2014**, *4*, 2369-2373.
22 (b) Li, G.; Jin, R. *J. Am. Chem. Soc.* **2014**, *136*, 11347-11354. (c) Vasilikogiannaki, E.;
23 Titilas, I.; Vassilikogiannakis, G.; Stratakis, M. *Chem. Commun.* **2015**, *51*, 2384-2387.
24 (d) Mitsudome, T.; Yamamoto, M.; Maeno, Z.; Mizugaki, T.; Jitsukawa, K.; Kaneda, K.
25 *J. Am. Chem. Soc.* **2015**, *137*, 13452-11354.
26 [12] (a) Sárkány, A.; Révay, Zs. *Appl. Catal. A: Gen.* **2003**, *243*, 347-355. (b) Vilé, G.;
27 Baudouin, D.; Remediakis, I. N.; Copèret, C.; López, N.; Pèrez-Ramírez, J.
28 *ChemCatChem* **2013**, *5*, 3750-3759. (c) Oakton, E.; Vilé, G.; Levine, D. S.; Zocher, E.;
29 Baudouin, D.; Pèrez-Ramírez, J.; Copèret, C. *Dalton Trans.* **2014**, *43*, 15138-15142.
30 [13] For the formation of PdH from the treatment of Pd NPs with H₂, see: (a) *Hydrogen*
31 *in Metals II*, (Eds.: G. Alefeld, J. Völkl), Springer-Verlag, Berlin, **1978**, 73-155. (b)
32 Christmann, K. *Surf. Sci. Rep.* **1988**, *9*, 8-10. (c) Yamauchi, M.; Kobayashi, H.;
33 Kitagawa, H. *ChemPhysChem* **2009**, *10*, 2566-2576.
34 [14] For H₂-permeability of Ag, see: (a) Katsuta, H.; McLellan, R. B. *Scripta*
35 *Metallurgica* **1979**, *13*, 65-66. (b) Chou, I-M. *Am. J. Sci.* **1986**, *286*, 638-658. (c) Aoki,
36 Y.; Shi, L.; Sugimoto, T.; Hirayama, H. *Surface Science* **2010**, *604*, 420-423.
37 [15] We chose hydroxyapatite as support which results in highest efficiency among the
38 tested supports. See, Section 5 in the supporting information for details.
39 [16] It is reported that Pd-Ag alloy showed high selectivity for the semihydrogenation
40 of acetylene in excess ethylene where small ensemble sites of the Pd-Ag alloy are
41 effective. We prepared the Pd-Ag alloys with small ensemble sites and tested them in
42 the hydrogenation of **2** under the same reaction condition. The comparison between
43
44
45
46
47
48
49
50
51
52
53
54
55
56
57
58
59
60

Pd@Ag and the Pd-Ag alloys was discussed, see the section 6 comparison between Pd@Ag and conventional catalysts in the Supporting Information. For Pd-Ag alloy in semihydrogenation, see: (a) Johnson, M. M.; Walker, D. W.; Nowack, G. P. (Phillips Petroleum Company), US 4404124, **1983**. (b) Thanh, C. N.; Didillon, B.; Sarrazin, P.; Cameron, C. (Institut Francais du Petrole), US 5648578, **1997**. (c) Zhang, Q.; Li, J.; Liu, X.; Zhu, Q. *Appl. Catal. A: Gen.* **2000**, *197*, 221-228. (d) Lamb, R. N.; Ngamson, B.; Trimm, D. L.; Gong, B.; Silveston, P. L.; Praserttham, P. *Appl. Catal. A: Gen.* **2004**, *268*, 43-50. (e) Zea, H.; Lester, K.; Datye, A. K.; Rightor, E.; Gulotty, R.; Waterman, W.; Smith, M. *Appl. Catal. A: Gen.* **2005**, *282*, 237-245. (f) Huang, W.; Pyrz, W.; Lobo, R. F.; Chen, J. G. *Appl. Catal. A: Gen.* **2007**, *333*, 254-263. (g) Lamberov, A. A.; Il'yasov, S. R.; Gil'manov, Kh.; Trifonov, S. V.; Shatilov, V. M.; Ziyatdinov, A. Sh. *Kinet. Catal.* **2007**, *48*, 136-142. (h) Ahn, I. Y.; Lee, J. H.; Kim, S. K.; Moon, S. H. *Appl. Catal. A: Gen.* **2009**, *360*, 38-42. (i) Lee, J. H.; Kim, S. K.; Ahn, I. Y.; Kim, W.-J.; Moon, S. H. *Catal. Commun.* **2011**, *12*, 1251-1254. (j) Pachulski, A.; Schödel, R.; Claus, P. *Appl. Catal. A: Gen.* **2011**, *400*, 14-24. (k) Zhang, Y.; Diao, W.; Williams, C. T.; Monnier, J. R. *Appl. Catal. A: Gen.* **2014**, *469*, 419-426. (l) Pei, G. X.; Liu, X. Y.; Wang, A.; Lee, A. F.; Isaacs, M. A.; Li, L.; Pan, X.; Yang, X.; Wang, X.; Tai, Z.; Wilson, K.; Zhang, T. *ACS Catal.* **2015**, *5*, 3717-3725.

[17] (a) Cormack, D.; Pritchard, J.; Moss, R. L. *J. Catal.* **1975**, *37*, 548-552. (b) Han, Y.; Peng, D.; Xu, Z.; Wan, H.; Zheng, S.; Zhu, D. *Chem. Commun.* **2013**, *49*, 8350-8352.

[18] Lee, T. W.; Kim, K.; Kim, M. S. *J. Mol. Struct.* **1992**, *274*, 59-73.

Graphic Abstract

